

THE OFFICIAL MAGAZINE OF THE OCEANOGRAPHY SOCIETY

Oceanography

CITATION

Hautala, S., H.P. Johnson, M. Pruis, I. García-Berdeal, and T. Bjorklund. 2012. Low-temperature hydrothermal plumes in the near-bottom boundary layer at Endeavour Segment, Juan de Fuca Ridge. *Oceanography* 25(1):192–195, <http://dx.doi.org/10.5670/oceanog.2012.17>.

DOI

<http://dx.doi.org/10.5670/oceanog.2012.17>

COPYRIGHT

This article has been published in *Oceanography*, Volume 25, Number 1, a quarterly journal of The Oceanography Society. Copyright 2012 by The Oceanography Society. All rights reserved.

USAGE

Permission is granted to copy this article for use in teaching and research. Republication, systematic reproduction, or collective redistribution of any portion of this article by photocopy machine, reposting, or other means is permitted only with the approval of The Oceanography Society. Send all correspondence to: info@tos.org or The Oceanography Society, PO Box 1931, Rockville, MD 20849-1931, USA.



Low-Temperature Hydrothermal Plumes in the Near-Bottom Boundary Layer at Endeavour Segment, Juan de Fuca Ridge

BY SUSAN HAUTALA, H. PAUL JOHNSON, MATTHEW PRUIS, IRENE GARCÍA-BERDEAL, AND TOR BJORKLUND

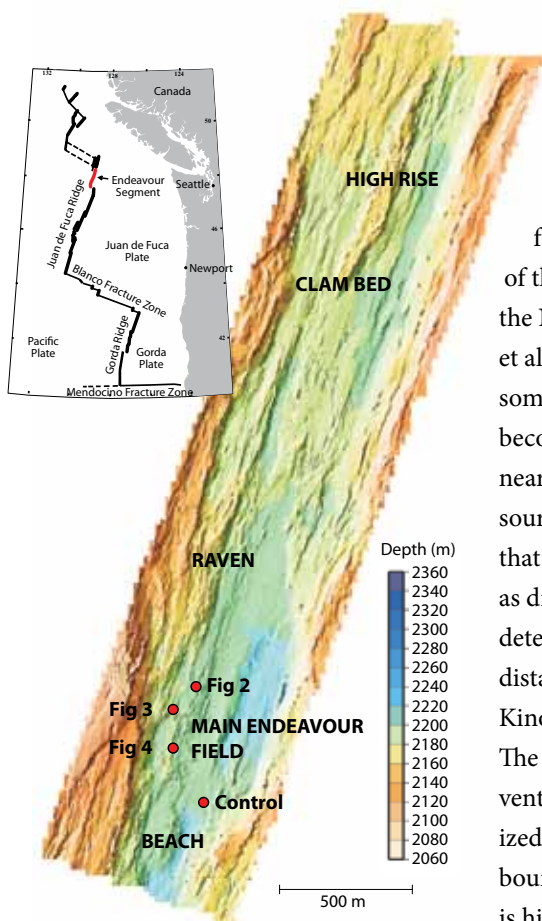


Figure 1. Map of the area of Endeavour Segment of the Juan de Fuca Ridge studied during the 2000–2003 Thermal Grid project, along with locations of instruments shown in Figures 2–4. The color bar indicates depth (m), determined by a *Jason 2* SM2000 swath bathymetry survey using a systematic grid. For more details, see Johnson et al. (2002).

Low-temperature (typically 5–75°C) fluid, commonly referred to as “diffuse” hydrothermal flow, emanates from fractures over a significant portion of the Juan de Fuca Ridge seafloor in the Northeast Pacific Ocean (Kelley et al., 2012, in this issue). Although some fraction of the diffuse effluent becomes entrained relatively quickly into nearby plumes from high-temperature sources, a number of studies suggest that a significant portion flows laterally as discrete low-level plumes that remain detectable downstream for considerable distances (Trivett and Williams, 1994; Kinoshita et al., 1998; Veirs et al., 2006). The seafloor near diffuse hydrothermal vents supports densely populated, localized biological communities in a bottom boundary layer (BBL) environment that is highly variable in both space and time. Currents, temperature, and turbulence in the BBL, in addition to a complex array of biological, chemical, geological, and other physical factors, influence community structure near diffuse vents. Tides strongly affect the flow direction

of both high-temperature (Veirs et al., 2006) and diffuse (Kinoshita et al., 1998) plumes within the water column, and have been observed to affect temperature in the immediate vicinity of diffuse vents (Little et al., 1988; Tivey et al., 2002; Sheirer et al., 2006). Here, we describe recent measurements that reveal in greater detail the important role that tidal advection plays in modulating the BBL environment near diffuse hydrothermal plumes.

From 2000–2003, the Thermal Grid project (Johnson et al., 2002; see Figure 1) used MAVS3 acoustic current meters, equipped with one-meter-long thermistor strings, to collect multiday time series of near-bottom temperature, vertical temperature gradient, three-component velocity, and turbulent heat flux. Sixteen low-temperature vent sites were sampled (see examples in Figures 2 to 4), ranging from South Main Endeavour to High Rise vent fields, along with a central axial valley control site where the near-bottom temperature is homogeneous within the thermistors’ accuracy of 0.02°C. Current

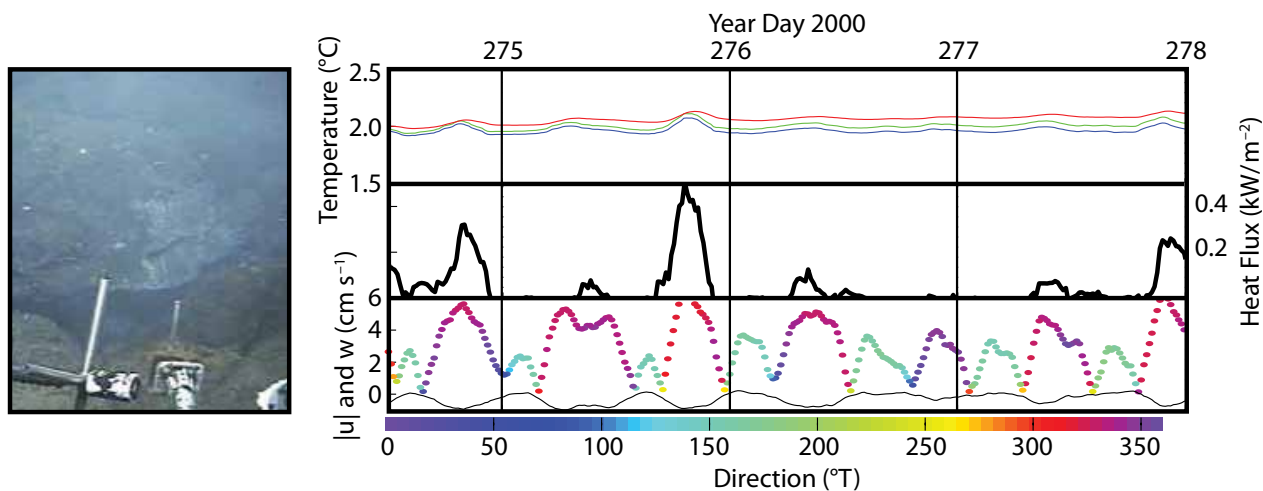


Figure 2. Record from a site located about 40 m west-southwest of the black smoker Hulk. On September 30, 2000, the instrument was deployed 7 m along bearing 304° from the diffusely venting crack shown at the left. Time (x-axis) is in GMT. The upper panel shows temperature at the bottom (red), at 0.5 m altitude (green), and at 1 m altitude (blue). Heat flux (center panel) is calculated via direct correlation, using ~ 2 Hz vertical velocity and temperature data, averaged over 17 minute ensembles. Data for all panels of the figure are further smoothed with a running mean over 10 ensembles. The lower panel shows horizontal current speed, color-coded by direction (°T = degrees clockwise from north), and vertical velocity (black). At this site, the current record is dominated by the semidiurnal tide with flow alternating direction along $335^\circ \pm 9^\circ$ during four periods of strong flow each day. Vertical velocity is also tidally modulated due to reversing flow oriented along a sloping bottom. Water from the diffuse source is swept past the sensor when the tidal current is to the northwest, resulting in a 0.05–0.2°C increase in temperature throughout the BBL, and vertical turbulent heat flux values of 0.1–0.5 kW m⁻². The record mean heat flux (with 95% confidence limit error using number of degrees of freedom determined from the integral time scale at the control site) is 0.04 ± 0.04 kW m⁻².

meter accuracy is 0.3 cm s^{-1} . Thermistor and velocity precisions are, respectively, 0.01°C and 0.03 cm s^{-1} , leading to an instrumental precision for heat flux of 12 W m^{-2} .

Strong spatial variability in the near-bottom boundary layer, defined here as the lowest one meter of the water column, begins at the water-rock interface. In a separate experiment, an array of 12 thermistors in contact with the seafloor, arranged in a triangle with 1 m

sides, yielded gradients of up to 10°C over fewer than 20 cm laterally, yet there was no visual indication of this variation in either seafloor appearance or tube-worm community health (Pruis, 2004). In the near-bottom boundary layer, spatial variability continues to be the norm. The orientations of both steady and oscillatory currents, typically several centimeters per second in strength, are controlled by local, small-scale topographic features; diffuse patches

within a few meters of one another can flow in significantly different directions. In the face of the tidal currents we observed, water column particles, including larvae, can be swept across horizontal distances of several hundreds of meters, along with net displacement rates amounting to $1\text{--}2 \text{ cm s}^{-1}$ due to the strong lateral changes in current magnitude and direction within the BBL (García-Berdeal, 2006).

Over a matter of hours, changes in tidal currents often dramatically alter the entire physical environment of the near-bottom boundary layer at a given diffuse vent site, although the influence of the tides wanes as heat flux strength increases. At many sites of low to moderately strong diffuse flow (see Figure 3), as the current speed alternates between

Susan Hautala (hautala@uw.edu) is Associate Professor, School of Oceanography, University of Washington, Seattle, WA, USA. **H. Paul Johnson** is Professor, School of Oceanography, University of Washington, Seattle, WA, USA. **Matthew Pruis** is Research Scientist, NorthWest Research Associates, Redmond, WA, USA. **Irene García-Berdeal** was a graduate student in the School of Oceanography, University of Washington, Seattle, WA, USA. **Tor Bjorklund** is Oceanographer, School of Oceanography, University of Washington, Seattle, WA, USA.

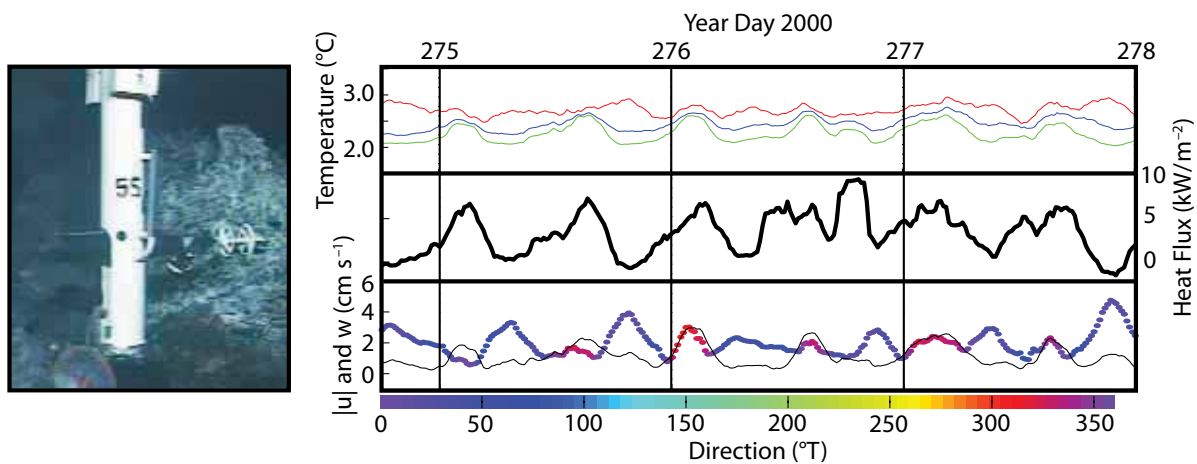


Figure 3. Information same as Figure 2 but for a deployment at the base of the talus slope about 34 m north of Grotto/Lobo vent, with the velocity sensor (white “ski-pole” end) sitting above the north flank of a small mound venting shimmering water and covered with tubeworms. The (usually) upper thermistor (blue) was unintentionally wrapped around the current meter and recorded values at a lower altitude than 0.5 m (green). In this location, the tide does not reverse the prevailing northward current, but periods of greatest heat flux are observed when the current is weakest, less than 1 cm s^{-1} to the north, and the buoyant plume can rise more vertically. The record mean heat flux is $3.4 \pm 1.1 \text{ kW m}^{-2}$. However, it is likely that the instrument did not sample the maximum heat flux—a temperature reading at the top of the mound reached $35^{\circ}\text{--}40^{\circ}\text{C}$.

maximum and slack tide, the BBL correspondingly shifts from situations where buoyant diffuse vent fluid is swept along the seafloor toward a regime where the diffuse plumes rise under their own buoyancy forces. These variations, associated with cycles in BBL temperature gradient, vertical velocity, and turbulent intensity, present the benthic community with diverse opportunities for and barriers to larval settlement and redistribution (García-Berdeal, 2006).

The vertical turbulent heat flux, measured at an altitude of 0.5 m above the bottom, also varies widely. Besides the control site, where the mean heat flux was less than the instrument precision, the lowest average heat flux observed was $0.04 \pm 0.04 \text{ kW m}^{-2}$, largely produced during discrete time intervals when the plume from a nearby source flowed past the sensor (Figure 2). Mean heat flux in excess of 10 kW m^{-2} was observed at 44% of the diffuse vent locations. Figure 3 shows a site with heat flux

close to the median value of 3.5 kW m^{-2} . At the high end, directly above a linear crack emitting white smoke, sustained values above 100 kW m^{-2} were observed (Figure 4).

Intermittency is observed in most records because the diffuse hydrothermal plume is strongly modulated—and sometimes only present—during one tidal phase. Temporal averaging of these records can, to some extent, substitute for spatial averaging around the vent field as the plume shifts from side to side over the tidal cycle. Still, estimating the total heat flux from a given source would require a sampling density sufficient to determine an accurate average value, along with a measure of the area of seafloor influenced by the diffuse plume. Furthermore, in particularly high heat flux and/or low current situations, the plume may separate from the near-bottom boundary layer, leading the turbulent flux calculation to underestimate heat flux. Nevertheless, to put our

measurements in context, Pruis (2004) extrapolates the median heat flux value we observed, assuming bounds of 0.5% to 5% for the fraction of the near-bottom boundary layer in Main Endeavour Field that is influenced by diffuse fluid, for an estimated low-temperature contribution of 6 to 58 MW. At the high end, this value represents about 10–20% of the total heat output of the field (Jonathan Kellogg, University of Washington, *pers. comm.*, 2011), and is comparable to an estimate of heat flowing laterally below 75 m altitude (Veirs et al., 2006). Venting at sites in between the principal vent fields, such as those we sampled at Beach, Clam Bed, and Raven, as well as other low-temperature sites yet to be discovered, augment the total diffuse hydrothermal heat flow from the segment.

While these observations, made over short windows of several days, provide insight into the effects of tidal currents on diffuse plumes in the near-bottom

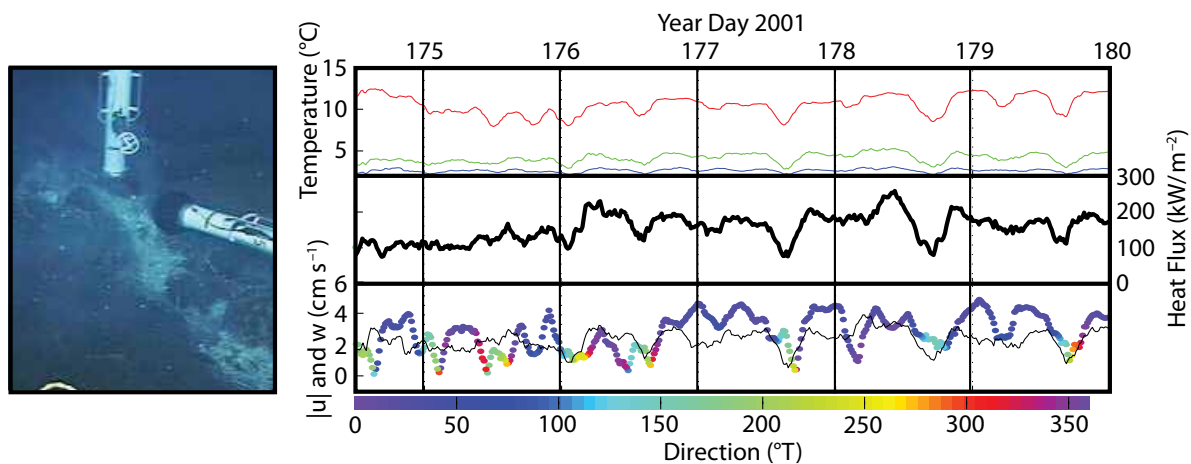


Figure 4. Information same as Figure 2 but for the strongest diffuse heat flux observed, at a site located approximately 40 m north-northwest of S&M vent, starting on June 23, 2001. The sensor is located 0.5 m above a linear crack oriented along approximately 060°. At this location, the combination of a northward background current and the semidiurnal tide results in only relatively brief periods of southward flow, accompanied by drops of several degrees in bottom temperature and a 50% reduction in the heat flux (record mean = $150 \pm 13 \text{ kW m}^{-2}$).

boundary layer, much work remains to be done to understand the physical controls on lower water column variability. And, many other factors are expected to be at play on different timescales, including tidal variability of the hydrothermal sources themselves, longer-period current variability, and the geophysical processes that control both the slow evolution/decay of diffuse vent systems and their responses to episodic seismic events.

Much more detailed discussion of the Thermal Grid project can be found in PhD dissertations by Matt Pruis (2004) and Irene García-Berdeal (2006), which can be accessed from the University of Washington ResearchWorks archive at: <https://digital.lib.washington.edu/researchworks>.

ACKNOWLEDGEMENTS

This work would not have been possible without the scientists and crew of R/V *Thompson* and

ROV *Jason 2*. Funding was provided by National Science Foundation grants OCE-9911523 and OCE-0085615 and the University of Washington Royalty Research Fund.

REFERENCES

- García-Berdeal, I. 2006. Hydrography and flow in the axial valley of the Endeavour Segment: Implications for larval dispersal. PhD Dissertation, University of Washington, Seattle.
- Johnson, H.P., S.L. Hautala, M.A. Tivey, C.D. Jones, J. Voight, M. Pruis, I. García-Berdeal, L.A. Gilbert, T. Bjorklund, W. Fredericks, J. Howland, and the Thermal Grid Scientific Party. 2002. A systematic examination of hydrothermal circulation: Endeavour Segment, Juan de Fuca Ridge. *Eos, Transactions, American Geophysical Union* 83:73, 78.
- Kelley, D.S., S.M. Carbotte, D.W. Caress, D.A. Clague, J.R. Delaney, J.B. Gill, H. Hadaway, J.F. Holden, E.E.E. Hooft, J.P. Kellogg, and others. 2012. Endeavour Segment of the Juan de Fuca Ridge: One of the most remarkable places on Earth. *Oceanography* 25(1):44–61, <http://dx.doi.org/10.5670/oceanog.2012.03>.
- Kinoshita, M., R.P. Von Herzen, O. Matsubayashi, and K. Fujioka. 1998. Tidally-driven effluent detected by long-term temperature monitoring at the TAG hydrothermal mound, Mid-Atlantic Ridge. *Physics of the Earth and Planetary Interiors* 108:143–154, [http://dx.doi.org/10.1016/S0031-9201\(98\)00092-2](http://dx.doi.org/10.1016/S0031-9201(98)00092-2).
- Little, S.A., K.D. Stolzenbach, and F.J. Grassle. 1988. Tidal current effects on temperature in diffuse hydrothermal flow: Guaymas Basin. *Geophysical Research Letters* 15:1,491–1,494, <http://dx.doi.org/10.1029/GL015i013p01491>.
- Pruis, M.J. 2004. Energy and volume flux into the deep ocean: Examining diffuse hydrothermal systems. PhD Dissertation, University of Washington, Seattle.
- Scheirer, D.S., T.M. Shank, and D.J. Fornari. 2006. Temperature variations at diffuse and focused flow hydrothermal vent sites along the northern East Pacific Rise. *Geochemistry Geophysics Geosystems* 7, Q03002, <http://dx.doi.org/10.1029/2005GC001094>.
- Tivey, M.K., A.M. Bradley, T.M. Joyce, and D. Kadko. 2002. Insights into tide-related variability at seafloor hydrothermal vents from time-series temperature measurements. *Earth and Planetary Science Letters* 202:693–707, [http://dx.doi.org/10.1016/S0012-821X\(02\)00801-4](http://dx.doi.org/10.1016/S0012-821X(02)00801-4).
- Trivett, D.A., and A.J. Williams III. 1994. Effluent from diffuse hydrothermal venting: 2. Measurements of plumes from diffuse hydrothermal vents at the southern Juan de Fuca Ridge. *Journal of Geophysical Research* 99:18,417–18,432.
- Veirs, S.R., R.E. McDuff, and F.R. Stahr. 2006. Magnitude and variance of near-bottom horizontal heat flux at the Main Endeavour hydrothermal vent field. *Geochemistry Geophysics Geosystems* 7, Q02004, <http://dx.doi.org/10.1029/2005GC000952>.